

Am I fit for this physical activity? Neural embedding of physical conditioning from inertial sensors

Davi Pedrosa de Aguiar
daviaguiar@dcc.ufmg.br
Universidade Federal de Minas Gerais
Belo Horizonte, Brazil

Otávio Augusto Silva
Universidade Federal de Minas Gerais
Belo Horizonte, Brazil
otavio.silva@dcc.ufmg.br

Fabricio Murai
Universidade Federal de Minas Gerais
Belo Horizonte, Brazil
murai@dcc.ufmg.br

ABSTRACT

Inertial Measurement Unit (IMU) sensors are becoming increasingly ubiquitous in everyday devices such as smartphones, fitness watches, etc. As a result, the array of health-related applications that tap onto this data has been growing, as well as the importance of designing accurate prediction models for tasks such as human activity recognition (HAR). However, one important task that has received little attention is the prediction of an individual's heart rate when undergoing a physical activity using IMU data. This could be used, for example, to determine which activities are safe for a person without having him/her actually perform them. We propose a neural architecture for this task composed of convolutional and LSTM layers, similarly to the state-of-the-art techniques for the closely related task of HAR. However, our model includes a convolutional network that extracts, based on sensor data from a previously executed activity, a physical conditioning embedding (PCE) of the individual to be used as the LSTM's initial hidden state. We evaluate the proposed model, dubbed PCE-LSTM, when predicting the heart rate of 23 subjects performing a variety of physical activities from IMU-sensor data available in public datasets (PAMAP2, PPG-DaLiA). For comparison, we use as baselines the only model specifically proposed for this task, and an adapted state-of-the-art model for HAR. PCE-LSTM yields over 10% lower mean absolute error. We demonstrate empirically that this error reduction is in part due to the use of the PCE. Last, we use the two datasets (PPG-DaLiA, WESAD) to show that PCE-LSTM can also be successfully applied when photoplethysmography (PPG) sensors are available to rectify heart rate measurement errors caused by movement, outperforming the state-of-the-art deep learning baselines by more than 30%.

KEYWORDS

heart rate estimation, IMU sensors, photoplethysmography, neural networks

1 INTRODUCTION

In the recent years there has been an ever increasing usage of sensor-equipped devices, such as smartphones, smartwatches and fitness watches. These sensors can be used to track user behavior and health-related measurements. Among the most common types are the Inertial Measurement Units (IMU), composed primarily of accelerometers and gyroscopes. The use of photoplethysmography (PPG) sensors to track heart rate (HR) is also becoming ubiquitous, especially in devices targeting fitness conscious consumers, such as the Apple Watch, FitBit and Samsung SimBand [10].

The HR is an important metric for the blood circulation, which distributes oxygen, nutrients and hormones to cells in the whole body. This characteristic, along with the relative ease of monitoring in comparison to alternative metrics (stroke volume, oxygen uptake, hormone levels, etc.), leads to the wide use of the HR as a proxy for cardiac strain by both professionals and amateurs in endurance training [6]. To promote an effective fitness training, it is necessary to induce an optimal cardiovascular response, making it essential to model and predict individual HR responses. This task is quite challenging as, besides responding to physical activities, the HR

is influenced by a number of factors such as genetics, nutrition, environmental conditions, fitness and mood [6].

Several methods have been designed to model or predict the heart rate under the influence of physical activity. Most of them are based on differential equations [1, 4], Hammerstein and Wiener models [7] or Neural Networks [8, 21–23]. Among the latter, some predict many steps into the future [21, 23], and others use IMU signals as input [21, 22] but, to the best of our knowledge, only the model proposed in [21] does both.

Despite the recent advances in neural networks, the problem of multi-step heart rate estimation from IMU sensor data remains little explored. In this paper, we investigate neural architectures that could be used for this task. In order to benchmark our model, in addition to using the model from [21], we adapt a network proposed for a closely related task called Human Activity Recognition (HAR), where the goal is to identify the activity being performed by a person (e.g., running, walking, swimming) given some sensor data – mostly, IMU – as input. For HAR, Convolutional Neural Networks (CNNs) [9, 12] and Recursive Neural Networks (RNNs) [9] are amongst the best performing classes of models.

Based on the premise that different subjects will display different HR levels when performing the same exercises depending on their physical conditioning, we propose a novel neural architecture that attempts to encode that attribute given IMU and HR data collected from a previous, short-lived, activity performed by an individual. This attribute is extracted by a CNN network as a vector called the physical conditioning embedding (PCE). The PCE is used, in turn, to set the initial values of the hidden and cell states of an LSTM responsible for outputting the HR predictions. Henceforth, the proposed method is referred as PCE-LSTM.

Although PPG sensors for tracking heart rate are becoming more common, they are prone to measurement errors due to motion-related artifacts. In this case, data from other sensors can be used to correct the heart rate measurements. This task, called PPG-based heart rate estimation, has been explored in [10, 13, 15]. To show that the proposed architecture can also be used for this task, we adapt PCE-LSTM to incorporate the PPG signal as an additional input and show that it can also outperform the state-of-the-art in this task.

In summary, our main contributions are:

- (1) we propose of a new model to predict heart rate from IMU-sensor signals;
- (2) we compare our model to the only neural network devised for the same task [21] and to a minimally adapted model shown to perform well on the related task of HAR [9];
- (3) we conduct an ablation study of the contribution of the PCE sub-network in the performance our PCE-LSTM model; and

- (4) we show our model also outperforms the state of the art for the heart rate estimation from PPG data.

Outline. Section 2 describes datasets and pre-processing used in this work. Section 3 details the proposed method, PCE-LSTM, and the key hypothesis we investigate. Section 4 discusses the reference methods for the heart rate estimation task. Section 5 presents the evaluation results. The related work is reviewed in Section 6. Last, Section 7 discusses the significance and impact of this work.

2 METHODOLOGY

This work addresses the problem of predicting the heart rate H_t of an individual at time $t = 1, \dots$, given IMU sensor data gathered up to time t and HR values from an initial, short lived period, H_1, \dots, H_I , with $I < t$. We refer to this task as **IMU-based multi-step heart rate estimation**. For this study, we choose the PAMAP2 [11] and PPG-DaLiA [10] datasets, which are among the very few publicly available sets containing both IMU and HR signals from individuals performing a variety of activities. PPG-DaLiA also has data from PPG sensors, which is disregarded in this first task.

The case where PPG sensors are available (in addition to IMU) is then addressed in this work as a secondary prediction task, referred as **PPG-based multi-step heart rate estimation**. Since PPG data are heart rate measurements that can be perturbed by movement, this task consists of correcting such measurements based on IMU data. For this task, we use the (complete) PPG-DaLiA [10] and WESAD [14] datasets. We show that it is possible to adapt the architecture proposed for the first to the second task with minor changes.

Below we describe the datasets in more detail, along with the pre-processing techniques used throughout this work.

2.1 Datasets

The PAMAP2 Dataset [11] consists of data from 40 sensors (accelerometers, gyroscopes, magnetometers, thermometers and heart rate sensor) sampled at 100Hz of 9 individuals performing 18 different activities, ranging from rope jumping, cycling and running to laying down, sitting and standing. There is a single time series of sensor signals per individual, each performing a sequence of activities. Later on we explain that the time series for 1 of 9 the individuals is too short for training the models.

The PPG-DaLiA Dataset [10] is composed of signals from two devices, a chest-worn device which provides accelerometer and ECG data; and a wrist-worn device measuring the photoplethysmography (PPG) and triaxial acceleration, sampled at 32 Hz. It also includes heart rate series computed from the ECG signals. This dataset contains a contiguous time series of sensor signals from 15 individuals performing 8 activities. We create a variant of this dataset, hereby referred simply as **the DaLiA dataset**, which does not include the PPG signals to use in the IMU-based multi-step HR estimation task.

The WESAD Dataset [14] consists of data from 15 subjects wearing the same sensors available in PPG-DaLiA, but differently from that dataset, the individuals remain seated/standing during the whole study while going through different affective states (neutral, stress, amusement), which are elicited by the use of funny video clips to bring about amusement, and the delivery of speeches to trigger stress. Unlike PPG-DaLiA, WESAD does not provide precomputed

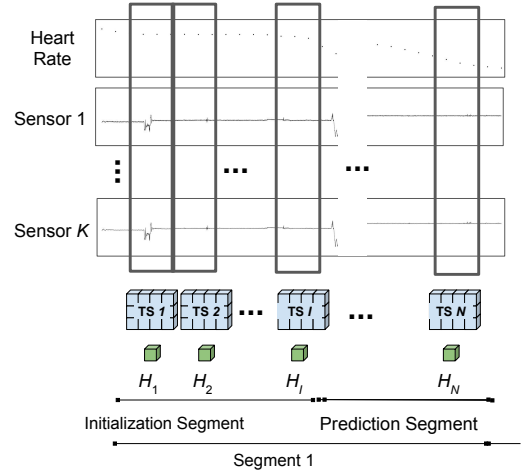


Figure 1: Time Snippet Representation

heart rate series, therefore we used the heartpy library [16] to extract heart rate measurements from the ECG signals. Although subjects are indexed up to number 17, the dataset does not include subject identifiers 1 and 12.

In total, we use data from 23 (resp. 30) individuals for the IMU-based (resp. PPG-based) multi-step heart rate estimation task.

2.2 Pre-processing

Basic Preprocessing. We upsample the heart rate signal using linear interpolation in all datasets to make its sampling rate consistent with the other signals. Only PAMAP2 contains a few missing data points, which we handle by local averaging the data around the missing point using a 0.4s window [2]. To make the use of the PAMAP2 and PPG-DaLiA datasets more consistent, we use only the accelerometer signals of the chest and wrist, and downsampled the signals to 32Hz. All signals s are z-normalized, i.e., $\hat{s} = (s - \mu(s))/\sigma(s)$, where μ stands for the mean operator and σ for the standard deviation operator.

Time Snippet Discretization. Like most works based on this data, we discretize the time series signals into **time snippets** (TS), i.e., partially overlapping windows of fixed duration τ_{TS} and overlap ratio r_{TS} (task-dependent). Figure 1 illustrates this procedure for the case when $r_{TS} = 0$. Each time snippet TS_t is a matrix where each row represents a sensor. Time snippets determine the granularity of the predictions. Accordingly, we define the average heart rate H_t for each time snippet TS_t as the response to be predicted.

Time Series Segmentation. In order to create a fixed-length training set, we segment the time series of each individual in a sequence of $N = 50$ contiguous time snippets of fixed duration. Hence, longer series can yield more segments. Each segment is partitioned into two smaller segments. The first, called **Initialization Segment**, contains the IMU and HR signals for the first $I = 12$ time snippets, and can be used by a neural network (NN) to encode a “state” specific to that time series. The second, called **Prediction Segment**, contains the IMU, but does not contain the HR, as it is used by a (possibly

different) NN to output predictions for each time snippet. Figure 1 illustrates the subdivision of a segment, in the case where $r_{TS} = 0$. Note that the NN used for processing the first segment can also be used for processing the second segment by replacing the HR signal in the latter by zeroes.

3 THE PHYSICAL CONDITIONAL EMBEDDING LSTM MODEL

Here we describe PCE-LSTM, our proposed neural network architecture for heart rate prediction. PCE-LSTM is composed of convolutional and LSTM layers, similarly to the state-of-the-art techniques for the closely related task of HAR. The novelty of this model is discussed below.

Recurrent Neural Networks (RNNs) have been especially designed to work with time series data. They are composed by cells with shared parameters, which process units of the input sequentially, using one or more vectors to carry state information through time. In particular, the unidirectional LSTM (long short-term memory) cell uses two vectors – the hidden state and the cell state – which are received from the previous iteration, updated based on the input for that time and passed onto the next iteration. The first iteration, however, receives these vectors as they were initialized, typically as zero vectors. The implicit assumption is that the network will gradually be able to encode the correct state from the inputs as the vectors are passed through the cells.

For HR prediction, we argue that if some data on the relationship between the input and output signals is available prior to the prediction, it can be beneficial to use a specialized network to encode this relationship as the RNN initial state. This initial state should contain information about physical conditioning: a more fit individual is able to sustain similar movement levels with smaller increase in HR. Thus, the main hypothesis investigated here can be stated as

***Hypothesis:** It is possible to encode information about physical conditioning from an individual’s sensor data as a vector and use it as the initial state of a RNN to improve heart rate predictions.*

This is the rationale behind the main difference between our approach and similar ones, namely the initialization of the RNN hidden vectors using a specialized network, which we call the Physical Conditioning Encoder.

Figure 2 shows the high level structure of our architecture, which is made of five components:

- the **Time Snippet Encoder** (TS Encoder), a convolutional network which encodes the 2-dimensional TS into a vector;
- the **Physical Conditioning Encoder** (PC Encoder), a convolutional network which extracts, from signals of the Initialization Segment (including heart rate), a Physical Conditioning Embedding (PCE) used for initializing the LSTM’s hidden vectors;
- the **Discriminator**, used for forcing the PCE of a given subject to be similar across time segments;
- the **State Updater**, a LSTM which maintains and updates the subject’s state, encoded in its hidden vectors; and
- the **Prediction Decoder**, a Fully-Connected network which decodes the heart rate prediction from the state tracked by the State Updater.

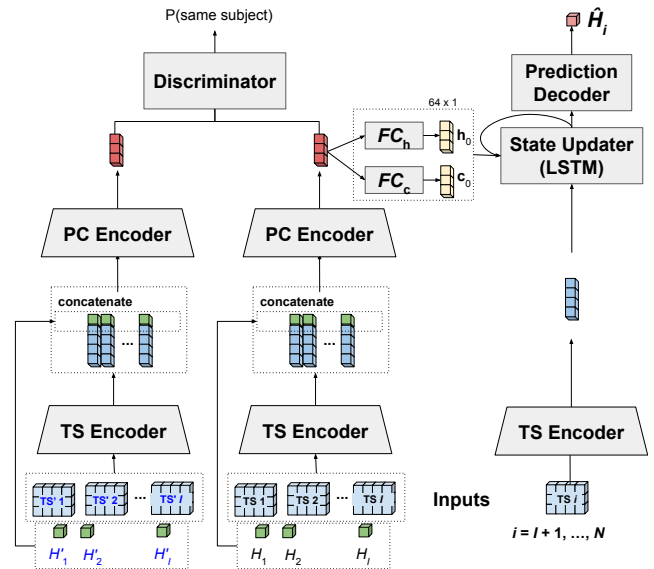


Figure 2: PCE-LSTM (proposed architecture).

Each component is described in detail below.

TS Encoder: extracts features from one time snippet. We reckon the role of each sensor in the description of the intensity of an activity as being equivalent to role of each RGB channel in the description of a picture. Hence, it is reasonable to combine them early in the NN. To do so, we use 1D convolutions along the time dimension, with the sensors stacked along the channel dimension. This approach differs from the most well known architectures in the literature [9, 10, 12], which keep the transformations on each sensor’s signals separate during the convolutional section of their architectures by the use of convolutional kernels spanning a single sensor, only combining them later on.

The TS Encoder comprises multiple layers, each made of a 1D convolution followed by a Leaky Rectified Linear Unit activation and a dropout layer of rate $TSE_{dropout}$. After each layer, the tensor length ℓ is reduced to $\lfloor \ell/2 \rfloor$ by filters of size 3 and stride 2 (when ℓ is even, we use padding = 1), except when the tensor length is 2, in which case we use a filter of size 2 without padding. All layers have TSE_F filters, except the last layer, which has TSE_{out} filters. The number of layers is $TSE_N = \lfloor \log_2(TS_L) \rfloor$, where TS_L is the length of the time dimension of the TS, so as to transform the size of the time dimension to one.

The vectors extracted from each time snippet of the Initialization Segment are concatenated along the time dimension, and the HR of each TS is concatenated along the feature dimension before being passed onto the next component.

PC Encoder: takes the vectors concatenated in the previous step and extracts a **physical conditioning embedding** (PCE). It is a multi-layer convolutional network that transforms the 2D-input ($(TSE_{out} + 1) \times D$) into a single vector of length PCE_{out} . PC Encoder is a convolutional architecture designed with the same principles as the TS Encoder. Figure 2 shows the PC Encoder in detail.

From the PCE, the LSTM’s hidden state vector and cell state vector are computed using a single linear layer each, represented in Figure 2 by FC_h and FC_c .

State Updater: is a standard LSTM with both state vectors (cell and hidden state’s) of size $LSTM_H$, and input of size TSE_{out} . These state vectors are initialized by the PC Encoder using only signals from the Initialization Segment. The LSTM is then fed with the deep attributes extracted by the TS Encoder from each time snippet.

Prediction Decoder: takes the hidden state representation for each time snippet from the State Updater and computes the prediction from these representations. It is made of three fully connected layers, where the first two layers have 32 neurons, each followed by a ReLU activation function, and the last layer have $LSTM_H$ neurons, without activation function, outputting the predicted HR. We use the mean absolute error (ℓ_1 loss) as the cost function L_{HR} associated with this output because using the ℓ_2 loss hampers training as larger differences between the predicted and actual heart rate have an out-sized impact on the loss, according to our preliminary experiments.

Discriminator: Regarding a subject’s physical conditioning as constant in the short term, we reason that employing a network to discriminate whether two PCEs belong to same person will foster better embeddings, when trained jointly with PCE-LSTM¹. To train the Discriminator, for each segment in the training set, we sample another segment from the same individual with probability 0.50 and from a different individual with probability 0.50. For each pair, we measure the cross entropy as the loss function (L_D). We set the weight of the discrimination loss to 10% of the total loss². Hence, the total loss L_{total} is given by

$$L_{total} = 0.9L_{HR} + 0.1L_D. \quad (1)$$

The Discriminator’s chosen architecture is comprised of 5 fully connected linear layers, each with 64 neurons and followed by ReLU activation function and a dropout rate of 0.15, except for the last layer, which uses a sigmoid activation function. This network receives two PCEs (concatenated) and outputs a probability .

3.1 Adaptations for PPG-based HR Estimation

The task of PPG-based HR estimation has three main distinctions from the IMU-only HR estimation and hence requires a few adaptations to our method. First, the PPG signal is better represented in the frequency domain; second, the PPG signal is more important than the other signals since it is a rough estimate of the HR; third, for PPG-based HR estimation, a ground truth HR is not usually available. In order to deal with these differences, we modified the TS Encoder sub-network to comprise two TS Encoder architectures, one for the raw PPG and IMU signals (TSE_{raw}) and another for the Fast Fourier the Transformed PPG signal ($TSE_{PPG-FFT}$). These outputs are concatenated and returned by the new sub-network. The $TSE_{PPG-FFT}$ is smaller, with $[TSE_{PPG-FFT}]_{out} = 12$. We also modified the PC Encoder slightly, so that it only receives as input the concatenated

¹We avoid overfitting to subjects in the training set by using different subjects in the validation set.

²Alternatively, the losses’ weights can be set by hyperparameter tuning, but since we use a single individual for validation, we fixed the weights to (0.9, 0.1) to avoid overfitting to the validation subject.

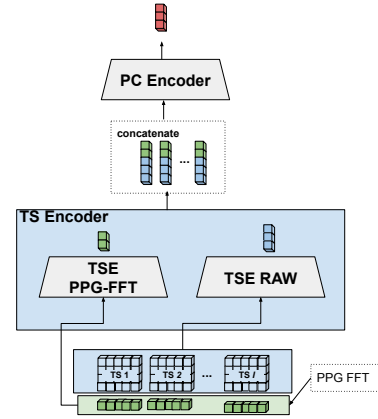


Figure 3: PPG-adapted PCE

outputs of the TSE (without the HR). Figure 3 illustrates the changes to the PCE-LSTM architecture for the secondary task.

4 REFERENCE METHODS

To the best of our knowledge, the task of predicting multiple steps of heart rate given IMU signals has only been attempted by [21], which used in their experiments a dataset not publicly available. In addition to using their model as a baseline, we also adapt a model designed for similar tasks (HAR) in order to benchmark our method. In this section we describe each of these models, the task they were designed to address and the minor changes required to adapt the models for the task at hand. More recent architectures for the HAR task, such as [12], were not used as baselines because they were not designed for multi-step predictions over time series and, as such, would require significant changes.

FFNN [21] is the only model in the literature proposed for HR prediction from IMU sensor data. Nonetheless, this model was applied only to a dataset not publicly available comprising a single time series of one individual performing normal daily activities, for which some promising results were reported. FFNN is a feed-forward recursive architecture with skip connections using data from a wrist-worn triaxial accelerometer. The model used the average measurement of each sensor in a non-overlapping window of 30s. As the architecture details were not reported we set the layer size to 16 and ReLU as the activation function for each layer based on random search optimization. We adapted their architecture, using a time window of $\tau_{TS} = 4s$, to make it more comparable to our method (testing with $\tau_{TS} = 30s$ as in the original work yielded worse results). We also used the Adam optimization algorithm for network weight optimization, instead of the genetic algorithms used in that study. Figure 4 illustrates the architecture.

DeepConvLSTM [9] is an architecture designed for the HAR task. It performs a sequence of convolutions on the input series, with padding adjusted so as to keep the dimensions of the tensor the same. The deep features from each time entry feed a LSTM. From each of the LSTM’s hidden vectors, a prediction is computed using a single linear layer. In our adapted version, we select only the outputs corresponding to the last time input of each time snippet, as we have one label per time snippet. As in the original article,

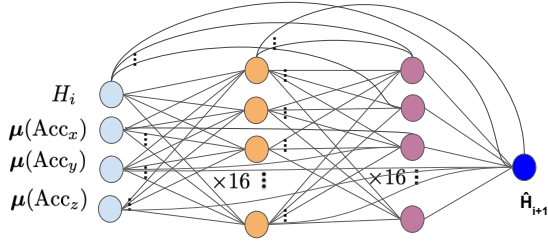


Figure 4: FFNN adapted architecture

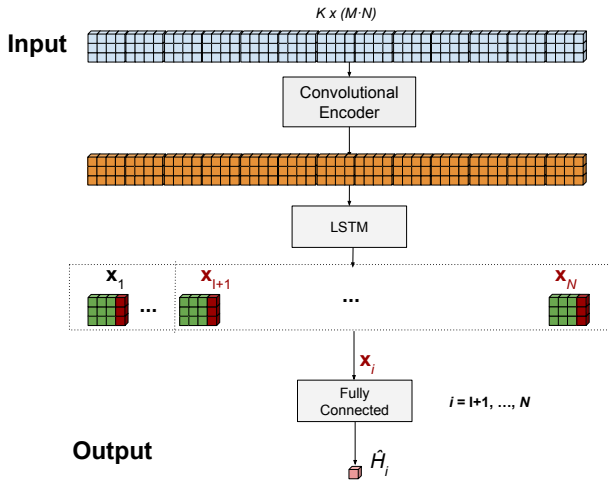


Figure 5: DeepConvLSTM architecture

we downsampled the input signals to 30Hz, and set time snippets’ length to $\tau_{TS} = 3s$. Figure 5 depicts the adapted architecture.

5 EMPIRICAL EVALUATION

In this section we describe the experiments conducted to evaluate PCE-LSTM and their results. We begin with an overview of the experimental setup. Next, we present the IMU-based HR prediction experiments (the primary prediction task) and an ablation study on PCE’s impact on performance. Last, we describe the PPG-based HR estimation (the secondary prediction task).

5.1 Experimental setup

For evaluating the IMU-based multi-step HR estimation results, we use both the Mean Absolute Error (MAE) and the Root Mean Squared Error (RMSE) as evaluation metrics. For the PPG-based HR estimation, however, we consider only MAE, since we transcribe the results from the paper where the baseline method was proposed [10], which did not include another evaluation metric.

Train-test split. Since the goal of this work is to predict an individual’s HR before he performs a physical activity, we create several train-test splits using a “leave one subject out strategy”. This mimics a realistic setting where the model would be applied to individuals not contained in the training set, as is the case for most models

trained offline [5]. In a dataset with S subjects, each of the subjects is used once as the test subject and the remaining $S - 1$ subjects’ time series are split into training segments of $N = 50$ time snippets each and then randomly assigned to Train/Validation sets using an 80/20 split. With each of the S subjects as the test subject, we perform 7 executions, with different Train/Validation splits and different neural network weight initialization, as done in [10].

Hyperparameter Tuning. In order to choose PCM-LSTM’ and the optimizer’s (Adam) hyperparameters, we applied a random search using the results on PAMAP2’s subject 5 as reference, following [9, 12], which used this subject for validation. The following hyperparameters were selected: $PCE_F = 64$, $I = 12$, $\tau_{TS} = 4$, $r_{TS} = 0.5$, $TSE_{out} = 128$, $TSE_F = 16$, $LSTM_H = 64$, $PCE_{out} = 64$, $TSE_{dropout} = 0.15$, learning rate = 5×10^{-3} , weight decay = 5×10^{-5} .

Training setup. All the models are optimized with Adam using the ℓ_1 loss as the cost function associated with the HR predictions. In each epoch, we compute the validation loss. After training is complete, we load the model weights that yielded the lowest validation loss. Training was done using a batch size of 64 over 100 epochs for PCE-LSTM and DeepConvLSTM. FFNN showed slower convergence and hence was trained for 200 epochs. Subject 9 of the PAMAP2 dataset was not included in the analysis because the corresponding time series is shorter than the length of the training segment (102s).

Mean vs. Ensemble performance. Since every method is trained 7 times for each test subject (using different train-validation splits), we compute a “mean” performance by averaging the errors of individual models and an “ensemble” performance by averaging the models’ predictions and then computing the resulting error, as done in [10].

Computational resources. All experiments were run on free Google Colab instances whose specs were Intel(R) Xeon(R) CPU@2.20GHz, 2 cores, 2 threads per core, Nvidia(R) Tesla T4 GPU, 12G RAM.

5.2 IMU-based multi-step heart rate estimation experiments

We begin by analyzing the results on the DaLiA dataset (without PPG data). Table 1 shows the Mean and the Ensemble performances w.r.t. the MAE for PCE-LSTM and the baselines, when the individual designated in the column is the test subject. The last column contains the row average. We note that the series of subjects 5 and 6 can be regarded as outliers as none of the methods performed well on them. As expected, ensembles tend to outperform their standalone counterparts. Considering the ensemble performances, out of 15 subjects, FFNN, DeepConvLSTM and PCE-LSTM achieve the lowest errors for 1, 2 and 12 subjects, respectively. The lowest average error is obtained by the PCE-LSTM ensemble (15.1% lower than FFNN and 18.2% lower than DeepConvLSTM). Table 2 shows the results of the same experiments w.r.t. RMSE metric. These results are consistent with those for the MAE (PCE-LSTM achieves an average error 16.9% lower than FFNN and 21.4% lower than DeepConvLSTM).

For a qualitative evaluation, we also plot the predictions of each model. Figure 6 shows the ensemble predictions for the complete

Model	Test Subject [beats/minute]															Avg.
	1	2	3	4	5	6	7	8	9	10	11	12	13	14	15	
FFNN (mean)	13.2	10.5	12.9	9.0	45.0	32.1	13.7	16.0	12.3	11.9	22.2	17.8	17.2	12.7	14.0	17.4
DeepConvLSTM (mean)	9.8	7.7	16.1	12.9	44.1	34.9	15.8	9.2	14.8	13.2	25.5	11.3	15.3	13.6	11.2	17.0
PCE-LSTM (mean)	9.3	6.5	12.2	8.7	42.0	34.7	11.3	12.2	13.6	12.2	22.4	15.1	10.9	11.5	9.2	15.5
FFNN (ens.)	12.2	8.0	11.4	7.7	45.0	31.4	12.4	14.5	11.5	8.6	22.1	17.3	15.0	11.2	10.6	15.9
DeepConvLSTM (ens.)	9.2	7.1	15.3	12.7	43.9	34.7	15.4	6.9	13.9	12.9	25.4	10.7	15.1	13.2	10.5	16.5
PCE-LSTM (ens.)	8.4	5.1	7.8	6.6	41.9	34.4	7.4	8.9	11.4	8.4	19.6	14.9	9.3	9.8	8.5	13.5

Table 1: Mean Absolute Error (beats/min) on the DaLiA dataset (best shown in bold)

Model	Test Subject [beats/minute]															Avg.
	1	2	3	4	5	6	7	8	9	10	11	12	13	14	15	
FFNN (mean)	16.1	13.5	16.5	11.2	50.2	37.5	19.1	21.9	18.3	17.5	26.2	20.0	23.1	17.8	17.5	21.8
DeepConvLSTM (mean)	13.8	11.0	19.2	15.6	47.5	39.6	21.0	12.0	21.0	17.4	30.1	14.3	21.1	18.8	15.5	21.2
PCE-LSTM (mean)	12.3	8.4	14.6	11.1	45.1	38.9	14.4	14.8	17.7	14.9	26.6	16.9	14.6	15.3	11.2	18.5
FFNN (ens.)	15.1	10.6	14.3	9.8	50.0	36.4	17.2	18.7	15.5	11.6	26.0	18.8	18.5	16.1	13.4	19.5
DeepConvLSTM (ens.)	13.2	10.3	17.7	15.1	47.4	39.2	20.6	9.4	20.5	17.2	29.9	13.5	21.0	18.5	14.7	20.6
PCE-LSTM (ens.)	11.0	6.8	9.5	7.9	44.7	38.6	10.5	10.5	15.8	11.6	23.1	16.2	12.9	13.7	10.2	16.2

Table 2: Root Mean Squared Error (beats/min) on the DaLiA dataset (best shown in bold)

series of five representative test subjects. We observe that DeepConvLSTM fails to capture the variance of the HR series: although the predictions are correlated with changes in HR, they tend to remain close to an “average” heart rate. FFNN, in turn, exhibits more variance, but cannot accurately capture the amplitude of the peaks and sometimes overestimates the HR. In contrast, PCE-LSTM (our method) can capture both peaks and valleys more accurately than the baselines, although it overestimates the HR for subject 12, similarly to FFNN.

We now turn our attention to the results on PAMAP2. Table 3 shows the Mean and the Ensemble performances w.r.t. the MAE for PCE-LSTM and the baselines, when the individual designated in the column is the test subject. The last column contains the row average. Not surprisingly, the ensembles yield better performance than the standalone models. Considering the ensemble performances, out of 8 subjects, FFNN, DeepConvLSTM and PCE-LSTM achieve the lowest errors for 1, 2 and 5 subjects, respectively. Once again, the lowest average error is obtained by the PCE-LSTM ensemble (33.2% lower than FFNN and 11.5% lower than DeepConvLSTM). Table 4 shows the results of the same experiments w.r.t. RMSE metric. We note a similar behavior: PCE-LSTM reduces the error by 33.9% in comparison to FFNN, and by 7.3% w.r.t. DeepConvLSTM.

Figure 7 shows the ensemble predictions for the complete series of five representative test subjects of the PAMAP2 dataset. In general, the observations are akin to those made for DaLiA: DeepConvLSTM produces the least variance, FFNN can capture some of the variance of the HR series, but PCE-LSTM most often outperforms the baselines at capturing peaks and valleys. Perhaps one exception to the last remark is seen on Subject 4’s time series between 2500 and 3000s, where the amplitude of the peak is better predicted by FFNN than by PCE-LSTM. Yet, note that none of the methods yields good results on this subject.

For a thorough comparison, we include some statistics related to the cost of each model in terms of memory and time resources. Table 5 shows the the number of parameters and training time required by each model, as well as the average time to compute a one-step prediction. Models sizes are larger for PAMAP2 dataset because it has more accelerometers on the chest and wrist than DaLiA. Thus, we include separate statistics for each dataset. We highlight that the execution time for all models, on Google Colab’s free servers, falls below the 2s interval required for online prediction.

5.3 Performance impact of PCE-LSTM’s hidden state initialization

In this section we conduct an ablation study to demonstrate that PCE-LSTM’s strategy for initializing hidden state vectors is key to boosting the model’s performance. A typical strategy to extract a hidden state is to use the LSTM itself to encode the relationship between sensor data and heart rate. In contrast, our model initializes the LSTM’s hidden state vectors by passing the sensor and heart rate data corresponding to the first $I = 12$ time snippets of the series through the Physical Conditioning Encoder (PC Encoder) to extract the embedding dubbed PCE. As we assume that the PCE encodes, at least in part, an individual’s physical conditioning, we expect that the joint training of the PCE-LSTM regression and the Discriminator will improve the regression predictions by promoting a better training of the PC Encoder subnetwork.

To quantify the performance impact of the proposed initialization and of using the discriminator, we conduct additional experiments with alternative initialization strategies. In what follows, “with discr.” indicates the joint training with the discriminator, “without discr.” indicates that the discriminator is not used; and “LSTM self-encode”, indicates that hidden state vectors are initialized by feeding the heart rate to the network as an additional input channel in the TS of

Model	Test Subject [beats/minute]								Avg.
	1	2	3	4	5	6	7	8	
FFNN (mean)	24.88	18.33	10.54	17.20	18.60	14.70	21.56	33.67	19.93
DeepConvLSTM (mean)	14.68	11.42	8.78	18.86	11.92	13.92	20.04	14.91	14.31
PCE-LSTM (mean)	16.59	10.75	9.02	19.50	9.56	9.91	12.63	14.92	12.86
FFNN (ensemble)	23.15	14.18	9.48	15.84	17.75	13.40	20.31	23.89	17.25
DeepConvLSTM (ensemble)	11.78	10.55	8.26	18.42	9.33	13.09	19.53	13.27	13.02
PCE-LSTM (ensemble)	16.46	9.46	8.34	16.70	8.40	8.80	10.79	13.25	11.52

Table 3: Mean Absolute Error (beats/min) on PAMAP2 (best shown in bold)

Model	Test Subject [beats/minute]								Avg.
	1	2	3	4	5	6	7	8	
FFNN (mean)	30.03	25.22	14.13	21.94	26.19	20.68	26.58	43.71	26.06
DeepConvLSTM (mean)	19.48	15.31	9.99	21.69	15.02	16.98	22.48	22.13	17.89
PCE-LSTM (mean)	19.76	14.38	12.89	23.50	12.70	12.64	16.09	19.47	16.43
FFNN (ensemble)	27.32	19.98	11.39	20.07	24.92	18.30	23.28	31.53	22.10
DeepConvLSTM (ensemble)	17.17	13.39	8.45	19.87	11.45	14.81	20.91	19.97	15.75
PCE-LSTM (ensemble)	19.36	12.99	11.80	19.51	10.61	11.11	14.04	17.40	14.60

Table 4: Root Mean Squared Error (beats/min) on PAMAP2 (best shown in bold)

Model	number of parameters	train. time [min]	execution time [ms]
DaLiA			
DeepConvLSTM	490,177	77.1	5.23
PCE-LSTM	120,273	20.4	0.20
FFNN	726	4.1	0.50
PAMAP2			
DeepConvLSTM	686,785	16.6	5.41
PCE-LSTM	120,561	5.1	0.14
FFNN	824	1.4	0.50

Table 5: Computational cost in number of parameters, training time and single-step prediction time

the Initialization Segment (replaced by zeros during the prediction segment).

Tables 6 and 7 show the MAE and RMSE metrics for these experiments on the DaLiA and PAMAP2 datasets, respectively. On DaLiA, PCE-LSTM’s outperforms an LSTM self-encode initialization strategy even without a discriminator. Nevertheless, the use of the discriminator reduces the error even further. On the other hand, on PAMAP2, PCE-LSTM without the discriminator yields larger error than the LSTM self-encode strategy. Even though the complete architecture – including the discriminator – achieves the lowest average error, the relative gains w.r.t. LSTM self-encode are marginal.

What can explain the difference between the results on the two datasets? To answer this question, we analyze the discrimination performance as a measure of the PCE’s quality. Figure 8 shows the discriminator accuracy for DaLiA and PAMAP2, respectively, when the threshold is set to 0.5 (i.e., the discriminator returns “same

person” when the predicted probability is above 50%). Although the overall accuracy is not very high, it is clear that it is higher on the DaLiA dataset, indicating that the resulting PCEs are more representative of the subjects’ physical conditioning. We conjecture the higher difficulty of encoding the physical conditioning on the PAMAP2 dataset might be due to its smaller size and larger number of activities being performed.

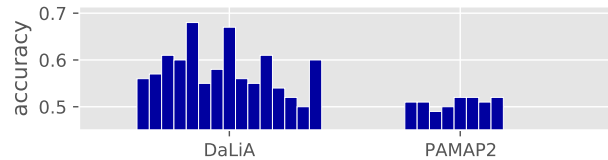


Figure 8: discriminator accuracy among test subjects in DaLiA and PAMAP2 datasets

5.4 PPG-based HR Estimation

We adapt PCE-LSTM for a secondary prediction task, namely, the PPG-based heart rate estimation. While being close to the IMU-based HR estimation the former task has been better explored in the literature and has, therefore, well established baselines. For this reason, we compare PCE-LSTM to the SOTA method based on deep learning [10]. This method is based on CNNs and will be referred simply as CNN.

In order to match the length and step size of each time snippet in [10], we set $\tau_{TS} = 8$ and $r_{TS} = 0.75$ for this task. Table 8 shows the ensemble performance for each method on PPG-DaLiA and WESAD, when the individual designated in the column is the test subject. The results of CNN ensemble method were transcribed directly from [10]. The last column contains the row average. On both

	Test Subject [beats/minute]															Avg.
	1	2	3	4	5	6	7	8	9	10	11	12	13	14	15	
	Mean Absolute Error															
LSTM self-encode (ens.)	11.0	7.6	7.1	7.4	48.6	33.6	10.7	15.6	11.5	9.3	21.2	15.2	10.7	10.7	10.4	15.4
without discr. (ens.)	10.5	5.9	13.7	7.6	43.7	29.5	7.8	14.3	9.4	9.5	18.8	13.6	9.1	11.4	7.7	14.2
with discr. (ens.)	8.4	5.1	7.8	6.6	41.9	34.4	7.4	8.9	11.4	8.4	19.6	14.9	9.3	9.8	8.5	13.5
	Root Mean Square Error															
LSTM self-encode (ens.)	13.6	9.6	9.1	9.0	50.9	38.0	14.2	18.6	16.5	12.5	24.2	17.7	13.5	14.2	12.3	18.3
without discr. (ens.)	12.9	7.3	15.4	9.4	46.3	33.8	10.7	16.1	13.7	12.6	22.3	14.7	11.7	15.6	9.5	16.8
with discr. (ens.)	11.0	6.8	9.5	7.9	44.7	38.6	10.5	10.5	15.8	11.6	23.1	16.2	12.9	13.7	10.2	16.2

Table 6: Ablation study: error results for variations of the PCE-LSTM model on DaLiA

	Test Subject [beats/minute]								Avg.
	1	2	3	4	5	6	7	8	
	Mean Absolute Error								
LSTM self-encode (ensemble)	14.60	11.27	7.92	13.43	7.90	9.95	13.83	14.17	11.63
without discr. (ensemble)	14.98	11.31	8.67	17.88	9.36	9.42	11.71	13.10	12.05
with discr. (ensemble)	16.46	9.46	8.34	16.70	8.40	8.80	10.79	13.25	11.52
	Root Mean Squared Error								
LSTM self-encode (ensemble)	17.51	14.86	10.94	16.53	9.86	12.33	16.19	19.32	14.69
without discr. (ensemble)	17.34	14.37	12.05	21.26	11.78	11.94	14.56	18.35	15.21
with discr. (ensemble)	19.36	12.99	11.80	19.51	10.61	11.11	14.04	17.40	14.60

Table 7: Ablation study: error results for variations of the PCE-LSTM model on PAMAP2

datasets, PCE-LSTM provides error reductions of approximately 32% when compared to the SOTA method. Another advantage of PCE-LSTM is that it has roughly two order of magnitude less parameters than the CNN – approx 120k parameters for PCE-LSTM vs. approx. 8500k parameters for the CNN model (according to [10]).

6 RELATED WORK

Few studies used IMU sensors to predict the heart rate (HR). [Yuchi and Jo \[22\]](#) used a simple Feed-Forward Neural Network to predict the HR one step ahead, given its value and the average signal of each IMU sensor on the previous step. Quite similarly, [Xiao et al. \[21\]](#) performed a multi-step HR prediction by repeatedly using the HR computed for step t to predict the HR for step $t + 1$. Their experiments demonstrated some promising results, but had some notable deficiencies, such as the use of data from a single individual in his daily activities, therefore without much variation in the HR values.

Also on multi-step HR estimation, but using speed and acceleration as inputs, [Zhang et al. \[23\]](#) proposed a Bayesian combined predictor, where one of the estimators was a linear regression and the other a neural network architecture similar to that of [21]. In their experiments, data from multiple individuals performing running sessions was used, thus addressing some of the shortcomings in [21]. However, the proposed method required calibration with actual HR data every 90s, hindering its practical use.

For HAR, a task where the use of IMU sensor data is widespread, [Hammerla et al. \[3\]](#) studied the performance of Deep Feed-Forward (DNN) Networks, CNN and Long-Short Term Memory (LSTM)

models, demonstrating that CNN and LSTM based models outperform DNNs and, among them, the best performing model was very dependent on the dataset used (for PAMAP2 [11], CNN was the best model).

A hybrid model, based on both CNNs and LSTM was devised by [Ordóñez and Roggen \[9\]](#). This model transforms the sensor signals using a CNN-based module and the output is then used to feed the LSTM. Although it achieved good results, the CNN-based architectures introduced by [Rueda et al. \[12\]](#) had higher performance in all analyzed datasets. More recently, some works proposed the use of self-attention based architectures for this task [17, 20]. The model proposed by [Rueda et al. \[12\]](#) outperformed the one proposed by [Vaswani et al. \[17\]](#) in the datasets that were common to both works. [Wu et al. \[20\]](#) proposed a deep attention model that was able to surpass [12] in some, but not all datasets. A more extensive survey was conducted by [Wang et al. \[19\]](#), where the authors note the variety of neural network architectures proposed for this task, in the literature, such as Convolutional Neural Networks, Deep fully-connected networks, Recurrent neural networks, Deep Belief Networks, Stacked Auto Encoders and hybrid approaches.

One of the difficulties in working with sensor data is the engineering of features. Multiple approaches are described in the literature. One of the simplest approaches was proposed by [Xiao et al. \[21\]](#), where features are the averages of each signal computed with a sliding window. [Walse et al. \[18\]](#) used the Principal Component Analysis (PCA) to extract features to be used for prediction. Due to the periodic nature of the signals, Fast Fourier Transforms were used

Am I fit for this physical activity? Neural embedding of physical conditioning from inertial sensors

		Test Subject (MAE [beats/min])														
Model	PPG-DaLiA															
	1	2	3	4	5	6	7	8	9	10	11	12	13	14	15	Avg.
CNN (ensemble) [10]	7.73	6.74	4.03	5.9	18.51	12.88	3.91	10.87	8.79	4.03	9.22	9.35	4.29	4.37	4.17	7.65
PCE-LSTM (ensemble)	5.53	3.77	2.54	5.41	10.96	5.54	2.61	9.09	6.57	2.62	5.47	8.47	2.73	3.71	3.36	5.22
Model	WESAD															
	2	3	4	5	6	7	8	9	10	11	13	14	15	16	17	Avg.
CNN (ensemble) [10]	5.07	14.48	7.84	7.7	3.88	6.78	4.27	3.99	8.89	11.07	6.52	5.26	4.18	12.78	9.36	7.47
PCE-LSTM (ensemble)	3.59	9.83	3.46	4.65	2.65	4.58	4.61	3.03	4.91	7.06	4.77	4.67	3.51	4.91	8.35	4.97

Table 8: PPG-based heart rate estimation experiments

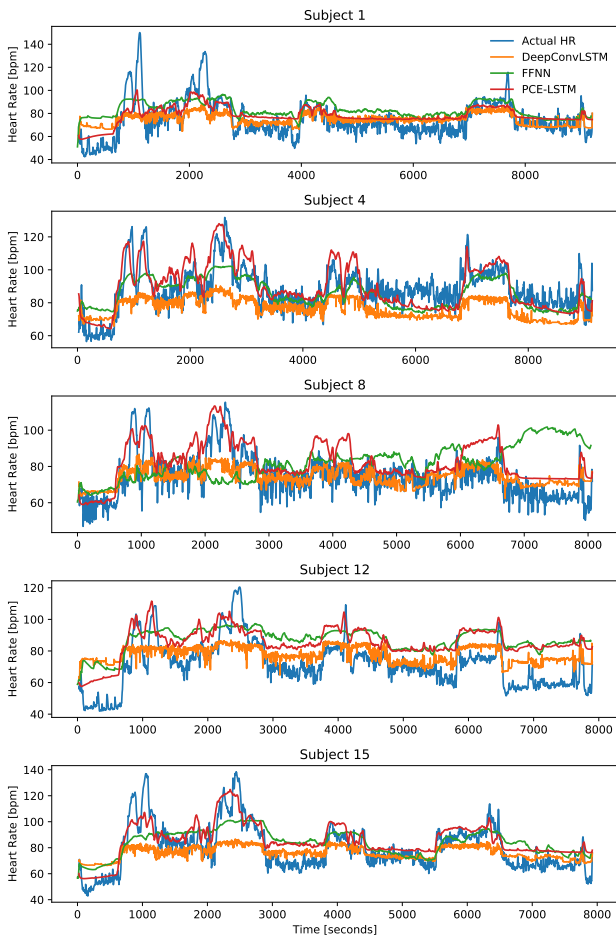


Figure 6: IMU-based HR estimation for entire series on DaLiA

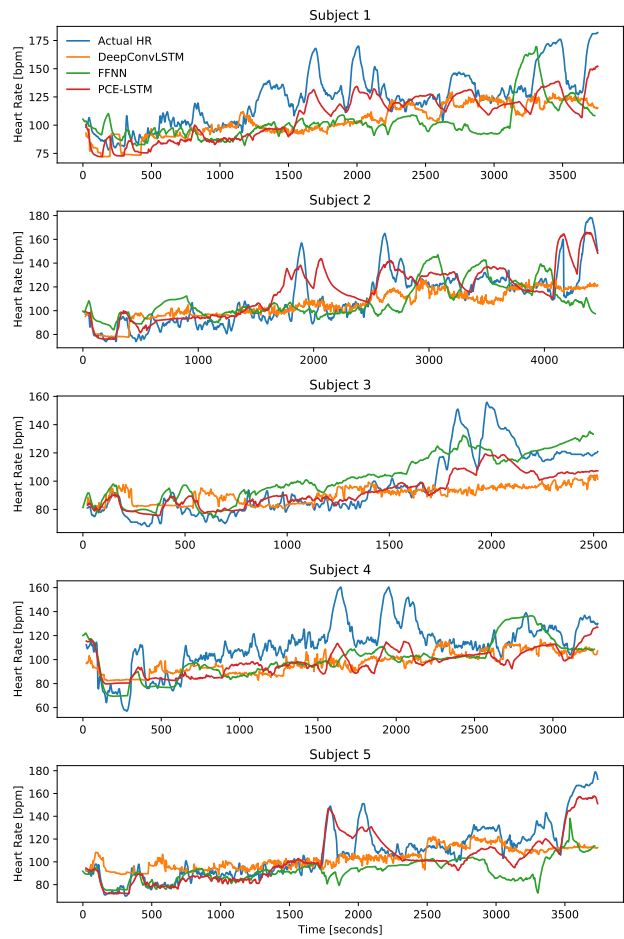


Figure 7: IMU-based HR estimation for entire series on PAMAP2

to extract the features in [2, 10]. Similarly to our work, [9, 12] used Convolutional Neural Networks directly on raw signals, avoiding the need of human expertise to design features.

7 CONCLUSIONS

In this work we investigated the – much neglected – task of predicting heart rate from IMU sensor data. We started from the premise that, depending on their physical conditioning, different people will display different heart rates when performing the same exercises. We

proposed a neural architecture dubbed Physical Conditioning Embedding LSTM (PCE-LSTM) that employs a convolutional network to extract vectors which carry information about the relationship between sensor measurements and the heart rate for a specific individual, thus representing his/her physical conditioning. These vectors are used as the initial state vectors for a LSTM network that outputs heart rate predictions from sensor data. We evaluate the prediction accuracy of PCE-LSTM w.r.t. the mean absolute error and root mean square error using sensor data from public datasets (PAMAP2, PPG-DaLiA, WESAD). Moreover, we compare PCE-LSTM with two baselines: one model proposed for this task (FFNN) and one minimally-adapted state-of-the-art model (DeepConvLSTM) originally proposed for the closely related task known as Human Activity Recognition.

PCE-LSTM yields over 10% lower mean absolute error in the IMU-based heart rate estimation task and 30% lower mean absolute error in PPG-based heart rate regression. Last, we conduct additional experiments to show that the performance gains achieved by our method are, in part, due to the strategy used to initialize the hidden vectors. Specifically, using the outputs of the PCE network applied to the data from the previous 12 time snippets of the subject's time series is helpful and works better than using the LSTM itself to output hidden vectors from the same data, specially when using physical conditioning embedding discriminator during training. As future work, we leave the investigation of other architectures to learn a physical conditioning embedding, and other architectures to be used as a complete pipeline, including more Attention Transformer models (increasingly regarded as the best architecture for sequential data).

REFERENCES

- [1] T. M. Cheng, A. V. Savkin, B. G. Celler, Lu Wang, and S. W. Su. 2007. A nonlinear dynamic model for heart rate response to treadmill walking exercise. In *IEEE IEMBS*. 2988–2991.
- [2] Odongo Steven Eyobu and Dong Seog Han. 2018. Feature representation and data augmentation for human activity classification based on wearable IMU sensor data using a deep LSTM neural network. *Sensors* 18, 9 (2018). <https://doi.org/10.3390/s18092892>
- [3] Nils Y Hammerla, Shane Halloran, and Thomas Plötz. 2016. Deep, convolutional, and recurrent models for human activity recognition using wearables. In *IJCAI*. 1533–1540.
- [4] Kenneth J Hunt and Andrzej JR Hunt. 2016. Feedback control of heart rate during outdoor running: A smartphone implementation. *Biomedical Signal Processing and Control* 26 (2016), 90–97.
- [5] Artur Jordao, Jr. Nazare, Antonio C., Jessica Sena, and William Robson Schwartz. 2018. Human Activity Recognition Based on Wearable Sensor Data: A Standardization of the State-of-the-Art. *arXiv e-prints*, Article arXiv:1806.05226 (June 2018), arXiv:1806.05226 pages. arXiv:1806.05226 [cs.CV]
- [6] Melanie Ludwig, Katrin Hoffmann, Stefan Endler, Alexander Asteroth, and Josef Wiemeyer. 2018. Measurement, Prediction, and Control of Individual Heart Rate Responses to Exercise—Basics and Options for Wearable Devices. *Frontiers in Physiology* 9 (2018), 778. <https://doi.org/10.3389/fphys.2018.00778>
- [7] Sami Mohammad, Thierry Marie Guerra, Jean Marie Grobois, and Bernard Hecquet. 2011. Heart rate control during cycling exercise using Takagi-Sugeno models. *IFAC Proceedings Volumes* 44, 1 (2011), 12783–12788. <https://doi.org/10.3182/20110828-6-IT-1002.01962>
- [8] Kusprasapta Mutijarsa, Muhammad Ichwan, and Dina Budhi Utami. 2016. Heart rate prediction based on cycling cadence using feedforward neural network. In *IEEE IC3INA*. 72–76.
- [9] Francisco Javier Ordóñez and Daniel Roggen. 2016. Deep convolutional and lstm recurrent neural networks for multimodal wearable activity recognition. *Sensors* 16, 1 (2016), 115.
- [10] Attila Reiss, Ina Indlekofer, Philip Schmidt, and Kristof Van Laerhoven. 2019. Deep PPG: large-scale heart rate estimation with convolutional neural networks. *Sensors* 19, 14 (2019), 3079.
- [11] A. Reiss and D. Stricker. 2012. Introducing a New Benchmarked Dataset for Activity Monitoring. In *IEEE ISWC*. 108–109. <https://doi.org/10.1109/ISWC.2012.13>
- [12] Fernando Moya Rueda, René Grzeszick, Gernot A Fink, Sascha Feldhorst, and Michael Ten Hompel. 2018. Convolutional neural networks for human activity recognition using body-worn sensors. *Informatics* 5, 2 (2018). <https://doi.org/10.3390/informatics5020026>
- [13] Seyed Salehizadeh, Duy Dao, Jeffrey Bolkhovskiy, Chae Cho, Yitzhak Mendelson, and Ki Chon. 2016. A Novel Time-Varying Spectral Filtering Algorithm for Reconstruction of Motion Artifact Corrupted Heart Rate Signals During Intense Physical Activities Using a Wearable Photoplethysmogram Sensor. *Sensors* 16, 1 (Dec 2016), 10. <https://doi.org/10.3390/s16010010>
- [14] Philip Schmidt, Attila Reiss, Robert Duerichen, Claus Marberger, and Kristof Van Laerhoven. 2018. Introducing WESAD, a Multimodal Dataset for Wearable Stress and Affect Detection. In *Proceedings of the 20th ACM International Conference on Multimodal Interaction (Boulder, CO, USA) (ICMI '18)*. Association for Computing Machinery, New York, NY, USA, 400–408. <https://doi.org/10.1145/3242969.3242985>
- [15] T. Schäck, M. Muma, and A. M. Zoubir. 2017. Computationally efficient heart rate estimation during physical exercise using photoplethysmographic signals. In *EUSIPCO*. 2478–2481.
- [16] Paul van Gent, Haneen Farah, Nicole van Nes, and Bart van Arem. 2019. Analysing noisy driver physiology real-time using off-the-shelf sensors: heart rate analysis software from the taking the fast lane project. *Journal of Open Research Software* 7, 1 (2019).
- [17] Ashish Vaswani, Noam Shazeer, Niki Parmar, Jakob Uszkoreit, Llion Jones, Aidan N Gomez, Łukasz Kaiser, and Illia Polosukhin. 2017. Attention is all you need. In *NeurIPS*. 5998–6008.
- [18] Kishor H Walse, Rajiv V Dharaskar, and Vilas M Thakare. 2016. Pca based optimal ann classifiers for human activity recognition using mobile sensors data. In *ICTIS: Volume 1*. Springer, 429–436.
- [19] Jindong Wang, Yiqiang Chen, Shuji Hao, Xiaohui Peng, and Lisha Hu. 2019. Deep learning for sensor-based activity recognition: A survey. *Pattern Recognition Letters* 119 (2019), 3–11.
- [20] Neo Wu, Bradley Green, Xue Ben, and Shawn O'Banion. 2020. Deep Transformer Models for Time Series Forecasting: The Influenza Prevalence Case. *arXiv e-prints*, Article arXiv:2001.08317 (Jan. 2020), arXiv:2001.08317 pages. arXiv:2001.08317 [cs.LG]
- [21] Feng Xiao, Ming Yuchi, Mingyue Ding, and Jun Jo. 2011. A research of heart rate prediction model based on evolutionary neural network. In *IEEE ICBMI*. 304–307.
- [22] Ming Yuchi and Jun Jo. 2008. Heart rate prediction based on physical activity using feedforward neural network. In *IEEE ICHIT*. 344–350.
- [23] Haibin Zhang, Bo Wen, and Jiajia Liu. 2018. The Prediction of Heart Rate During Running Using Bayesian Combined Predictor. In *IEEE IWCMC*. 981–986.